Water Air Soil Pollut (2018) 229: 53
https://doi.org/10.1007/s11270-018-3699-z

Effects of Synthesis Conditions on Characteristics of Ni/Fe Nanoparticles and Their Application for Degradation of Decabrominated Diphenyl Ether

Yunqiang Yi · Juan Wu · Yufen Wei · Zhanqiang Fang · Yanyan Gong · Dongye Zhao

Received: 30 October 2017 / Accepted: 11 January 2018 / Published online: 6 February 2018

Abstract Ni/Fe bimetallic nanoparticles have been widely used as strong reductants to degrade organic pollutants. Synthesis parameters of Ni/Fe nanoparticles can directly affect their characteristics and reactivity. In this study, Ni/Fe nanoparticles were prepared at different synthesis conditions, namely, synthesizing temperature, stirring rate, washing solutions, and preparation methods (post-coated and co-reducted Ni/Fe nanoparticles), and investigated their effectiveness of decabrominated diphenyl ether (BDE209) degradation. The results showed that the successive order of factors affecting the kinetics constant of Ni/Fe nanoparticles for the removal of decabrominated diphenyl ether (BDE209) were preparation methods, washing solutions, stirring rate, and synthesis temperature. It should be noted that the kinetics constants of post-coated Ni/Fe nanoparticles for removal of BDE209 was 0.049 min^{-1}, which was 14 times higher than that of co-reducted Ni/Fe nanoparticles. Moreover, the most remarkable influence on the particle size of Ni/Fe nanoparticles was the stirring rate, others synthesis conditions are mentioned in the following order: washing solutions > preparation methods > synthesis temperature. Interestingly, the effects of synthesis condition on the crystalline structure of Ni/Fe were weak. The results may facilitate more effective application of Ni/Fe nanoparticles for degradation of BDE209.

Keywords Ni/Fe bimetallic nanoparticles · Synthesis conditions · Polybrominated diphenyl ethers · Degradation

Y. Yi · J. Wu · Y. Wei · Z. Fang
School of Chemistry and Environment, South China Normal University, Guangzhou 51006, China

Y. Yi · J. Wu · Y. Wei · Z. Fang (✉)
Guangdong Technology Research Centre for Ecological Management and Remediation of Water System, Guangzhou 5100, China
e-mail: sunmoon124@163.com
e-mail: zhqfang@scnu.edu.cn

Y. Gong
School of Environment, Guangzhou Key Laboratory of Environmental Exposure and Health, Guangdong Key Laboratory of Environmental Pollution and Health, Jinan University, Guangzhou 510632, China

D. Zhao
Environmental Engineering Program, Department of Civil Engineering, Auburn University, Auburn, AL 36849, USA

1 Introduction

With the rapidly development of nanotechnology, artificial nanomaterials are increasingly applied to environmental restoration and remediation. Noteworthily, nanoscale zero-valent iron (nZVI) has been wildly used for remediation of a variety of environmental contaminants, such as heavy metal (Ponder and Mallouk 2000; Li and Zhang 2007; Wang et al. 2016), polychlorinated biphenyls (PCPs) (Chen et al. 2010; Petersen et al. 2012; Bae and Lee 2014), polybrominated diphenyl ethers (PBDEs) (Zhuang et al. 2010; Fang et al. 2011; Tan et al.

2017), and nitrate (Alowitz and Scherer 2002; Choe et al. 2004; Hu et al. 2016), due to its large specific surface area and strong reducibility. nZVI can effectively degrade halogenated organic pollutants via hydrodehalogenation or reductive dehalogenation (Chen et al. 2010; Zhuang et al. 2010; Fang et al. 2011; Petersen et al. 2012; Bae and Lee 2014). However, nZVI is easy to agglomerate during preparation and application, hence diminishing their reactivity. Nickel is a preferred doping metal with nZVI to form Ni/Fe bimetallic particles due to its low cost and potential as a catalyst to enhance the dehalogenation rate (Chun et al. 2010). Moreover, the presence of Ni on the nZVI surface effectively prevented the aggregation of nZVI particles and improved the reactivity (Tian et al. 2009; Yazdanbakhsh et al. 2016; Shen et al. 2017). For instance, Lin et al. (2015) reported that the dechlorination efficiency of pentachlorophenol (5 mg/L) using 4 g/L post-coated Ni/Fe nanoparticles (an average diameter of 100 nm) was 46% within 600 min under the optimal condition, compared to 13% by nZVI alone. Zhang et al. (2006)found that 2.5 g/L co-reducted Ni/Fe nanoparticles with an average particle size of 30 nm degraded 46% of 50 mg/L PCP within 30 min. Compared with nZVI, those studies confirmed that Ni/Fe bimetallic nanoparticles could improve the capacity of removal contaminant. At the same time, due to the differences of synthesis conditions during the preparation of Ni/Fe bimetallic nanoparticles, the reactivity of nanoparticles prepared by different investigators are also enormously distinction.

Synthesis conditions during the preparation of nanoparticles may result in nanomaterials with various physicochemical properties, such as particle size and crystal structure, which are very closely related to the reactivity of the nanoparticles (Li et al. 2006; Kim et al. 2013). Liou et al. (2006) investigated the influences of different precursor concentrations of $FeCl_3$ (1.0, 0.1and 0.01 M) on the characteristics of nZVI, and revealed that nZVI prepared under low precursor concentration (0.01 M) possessed the smallest particle size (9.5 nm at 0.01 M $FeCl_3$ vs. 40 nm at 0.1 M $FeCl_3$ vs. 45 nm at 1 M $FeCl_3$) and the greatest specific surface area, resulting in the highest reactivity towards nitrate. Hwang et al. (2011) found that the particle size of nZVI dramatically decreased from 87.4 to 9.5 nm under short reaction time and high reductant concentration (reductant delivery rate 20 mL/min and 358.5 mM $NaBH_4$), simultaneously, the specific surface area increased from 8.4 to 45.4 m^2/g, and the reactivity towards nitrate was also enhanced. In addition, findings from Woo et al. (2014) suggested that washing with volatile solvents and drying under aerobic condition should be recommended as effective processes to obtain nZVI with higher reactivity at reasonable costs and efforts. All the researches mentioned above emphasized that the synthesis conditions would be the key factors affecting the reactivity of nZVI; however, the effects of synthesis conditions on the characteristics of Ni/Fe bimetallic nanoparticles and their degradation reactivity towards BDE209 have not been sufficiently addressed.

In this study, Ni/Fe nanoparticles were prepared under different synthesis conditions including temperature, stirring rate, washing solvents, and preparation methods and compared for the characteristics via dynamic light scattering (DLS), X-ray diffraction (XRD), and zeta potential. The influences of synthesis conditions on the reactivity of Ni/Fe bimetallic nanoparticles were also evaluated by degradation kinetics of decabrominated diphenyl ether (BDE209).

2 Experimental Procedures

2.1 Chemicals

Decabrominated diphenyl ether (98%) was supplied by Aladdin (Shanghai, China); sodium borohydride, ferrous sulfate, nickel chloride, ethanol, and acetone were of analytical grade and purchased from Tianjin Kermel Chemical Reagent Development Center; and tetrahydrofuran and methanol were of chromatographically pure and obtained from Tianjin Kermel Chemical Reagent Development Center. All the chemicals in this study were used as received.

2.2 Preparation of Ni/Fe Nanoparticles with Different Synthesis Methods and Conditions

2.2.1 Preparation of Post-coated Ni/Fe Nanoparticles and Co-reducted Ni/Fe Nanoparticles

Post-coated Ni/Fe nanoparticles were prepared following a previously reported method (Lin et al. 2015). In

brief, 0.6 mol/L $NaBH_4$ solution was rapidly added into 0.144 mol/L $FeSO_4 \cdot 7H_2O$ dissolved in 100 mL ethanol/water (3:7) with preselected synthesis conditions under nitrogen purging. Five minutes later, the formed black particles (Fe^0) were separated by magnetic bar, washed with N_2-purged DI water and ethanol. Then, Fe^0 were re-dispersed in 50 mL ethanol solution, followed by the addition of 50 mL $NiCl_2 \cdot 6H_2O$. The mixture was stirred for another 30 min. The solid residues (Ni/Fe nanoparticles) were separated and washed following the same procedure as the preparation of Fe^0 and then vacuum dried overnight at 60 °C. The Ni/Fe nanoparticles were stored in air-tight container for further use.

Co-reducted Ni/Fe nanoparticles were synthesized following the method by (Zhang et al. 2006). Under otherwise identical synthesis conditions, $FeSO_4 \cdot 7H_2O$ and $NiCl_2 \cdot 6H_2O$ were first dissolved in 100 mL ethanol/water, and then $NaBH_4$ solution (0.6 mol/L, 50 mL) was rapidly added into the mixed solution. The resultant solid residues were treated following the same procedure as mentioned in the preparation of post-coated Ni/Fe.

2.2.2 Effects of Synthesis Conditions

Samples I, II, and III were conducted to determine the effects of synthesis temperature. Similarly, samples II, IV, and V were aimed at verifying the effects of stirring intensity. Then, the effects of washing solvents were investigated by varying the washing solvents in samples IV, VI, and VII. Lastly, the preparing methods of Ni/Fe bimetallic nanoparticles were also studied in samples IV and VIII. Through the theoretical calculation, the content of nickel in bimetallic nanoparticles were overall nearly 20.5 wt%. The Ni/Fe synthesized under different conditions were summarized and named in Table 1.

2.3 Characterization of Ni/Fe Nanoparticles

The hydrodynamic diameters and zeta potential of Ni/Fe particles were measured using a Zetasizer Nano ZS (Malvern Nano-ZS90). The crystalline structure of Ni/Fe bimetallic nanoparticles was determined using an X-ray diffraction (Y-2000, Dandong, China) with a Cu-Kα radiation. The accelerating voltage and applied current were 30 kV and 20 mA, respectively. XRD spectra were acquired over a 2θ range of 0°–80° with a scanning speed of 0.8°/s.

2.4 Reactivity of Ni/Fe Nanoparticles Towards BDE209

A 200-mg/L stock solution of BDE209 in tetrahydrofuran (THF) was prepared and stored in a refrigerator under 4 °C. The desired working concentration of BDE209 was diluted by the THF/water solution (Leal et al. 2013; Xie et al. 2014). A certain amount of Ni/Fe (4 g/L) synthesized under different conditions were added into 150-mL conical flasks with a stopper, which contained 100 mL BDE209 solution (initial concentration = 2 mg/L, initial pH = 6). The reactor was then sealed and stirred at 200 r/min at (28 ± 2)°C. At the predetermined time intervals, 1 mL supernatant was taken out by a glass syringe, filtered through 0.22-μm membrane filters, and then analyzed for BDE209 using a Shimadzu high-performance liquid chromatograph (HPLC) equipped with a UV-visible detector set at a wavelength of 240 nm. The detection limit was 1 μg/L and the relative standard deviations were less than 2%. The mobile phase was methanol with a flow rate at 1.2 mL/min (Fang et al. 2011; Xie et al. 2014).

Table 1 Ni/Fe prepared under different conditions

Sample	Synthesis methods	Stirring velocity (rpm)	Temperature (°C)	Washing solvents
I	Post-coated Ni/Fe nanoparticles	300	30	Deoxidizing water and ethanol
II	Post-coated Ni/Fe nanoparticles	300	40	Deoxidizing water and ethanol
III	Post-coated Ni/Fe nanoparticles	300	50	Deoxidizing water and ethanol
IV	Post-coated Ni/Fe nanoparticles	400	40	Deoxidizing water and ethanol
V	Post-coated Ni/Fe nanoparticles	500	40	Deoxidizing water and ethanol
VI	Post-coated Ni/Fe nanoparticles	400	40	Deoxidizing water
VII	Post-coated Ni/Fe nanoparticles	400	40	Ethanol
VIII	Co-reducted Ni/Fe nanoparticles	400	40	Deoxidizing water and ethanol

3 Results and Discussion

3.1 Effects of Synthesis Temperature

The influences of synthesis temperature on the reactivity and characteristics of Ni/Fe bimetallic nanoparticles were investigated in the range from 30 to 50 °C (the initial stirring rate was 300 r/min, washing solvents were deoxidizing water and ethanol) and the results were compared in Fig. 1. As time increased, the removal efficiency of BDE209 by Ni/Fe nanoparticles increased (Fig. 1a). After 10 min, the removal efficiency of BDE209 was 53.4, 78.9, and 69.2% for Ni/Fe prepared at synthesis temperature of 30, 40, and 50 °C, respectively. The removal efficiency reached approximately 100% after 180 min. The degradation data were fitted by pseudo-first-order kinetic model and the resultant kinetics constants (Supporting information) were 0.034, 0.045, and 0.042 min^{-1} for Ni/Fe prepared at 30, 40, and 50 °C, respectively, which illustrated that the influence of synthesis temperature of Ni/Fe on the removal of BDE209 was insignificant. When the synthesis temperature was 40 °C, the reactivity of Ni/Fe was the highest.

The hydrodynamic diameter distribution of Ni/Fe nanoparticles at various synthesis temperature is

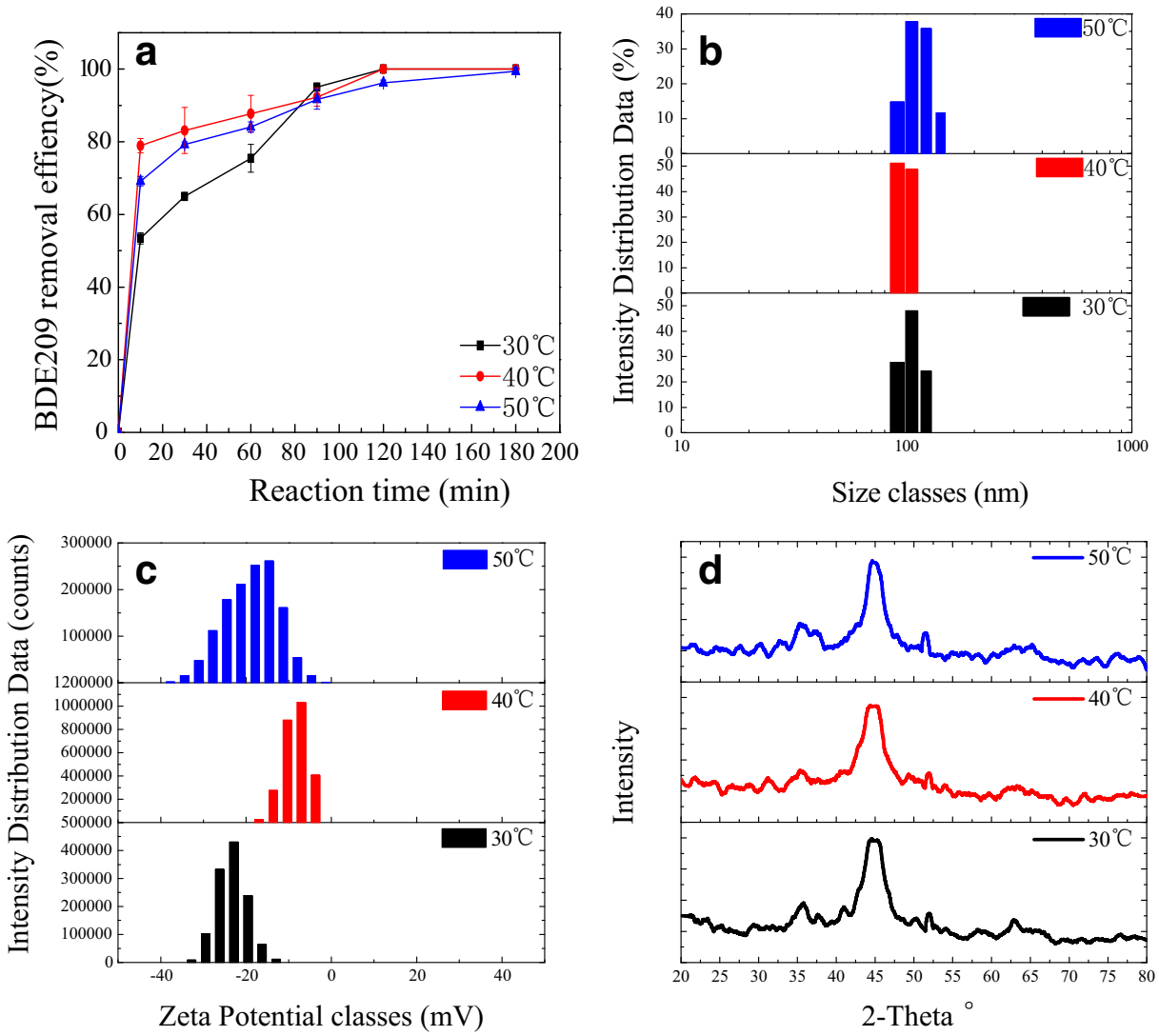

Fig. 1 Effects of synthesis temperature on the characteristics and reactivity of the Ni/Fe (removal efficiency (**a**), DLS particle size distribution (**b**), zeta potential (**c**), and XRD (**d**))

depicted in Fig. 1b. The hydrodynamic diameter of Ni/Fe nanoparticles prepared at 30 °C was measured to be 105.78 ± 1 nm, compared to 98.32 ± 0.8 nm at 40 °C. It should be noted that when the synthesis temperature further increased to 50 °C, the value moderately increased to 113.76 ± 2 nm. The hydrodynamic diameter distribution of Ni/Fe nanoparticles at various synthesis temperature is depicted in Fig. 1b. The hydrodynamic diameter of Ni/Fe nanoparticles prepared at 30 °C was measured to be 105.78 ± 1 nm, compared to 98.32 ± 0.8 nm at 40 °C. It should be noted that when the synthesis temperature further increased to 50 °C, the value moderately increased to 113.76 ± 2 nm. Obviously, the influences of synthesis temperature on the particle size of Ni/Fe were unremarkable. Zeta potential were − 18.82 mV (30 °C), − 21.21 mV (40 °C), and − 8.48 mV (50 °C), respectively (Fig. 1c). The minimum particle size and best stability of Ni/Fe nanoparticles were achieved when the synthesis temperature was 40 °C. The synthesis temperature can affect the reduction of $Fe^{2+}$and Ni^{2+}, nucleation of Fe atoms/clusters, and particle aggregation rate. Sodium borohydride and Fe^0 are strong reducing agents, and the reduction of Fe^{2+} and Ni^{2+} are fast processes under mixing. The change in temperature should not alter the reduction rate to any significant extent. Therefore, the temperature mainly affect nucleation and particle aggregation rate (He and Zhao 2007). Yang et al. (2014) reported a similar temperature effect on particle size of Ag nanoparticles, and they noticed that the formation of Ag nanoparticles was easy to aggregate at lower temperature, inducing larger particle size of nanoparticles while higher temperature could accelerate this process and triggered off the following reaction quickly, which shorten the time for the growth of micelles and higher temperature might enhance Brownian movement and broaden the micelle size distribution by combination of neighboring micelles. Meanwhile, XRD patterns (Fig. 1d) of Ni/Fe nanoparticles presented similar broad peaks at $2\theta = 44.9°$ for crystalline Fe^0 with severe background noises (Kim et al. 2013), regardless of synthesis temperature, indicated that amorphous structure of Ni/Fe bimetallic nanoparticles should not be significantly varied by synthesis temperature; however, an additional peak appeared at 35.6° on the particles, indicating the formation of γ-Fe_2O_3 or Fe_3O_4 during the characterization and preparation of Ni/Fe, a similar outcome has been confirmed elsewhere (Fang et al. 2011; Weng et al. 2013).

3.2 Effects of Synthesis Stirring Rate

Effects of stirring rate on the reactivity and characteristics of Ni/Fe bimetallic nanoparticles were investigated by fixing the synthesis temperature (40 °C) and the washing solutions (deoxidizing water and ethanol). As shown in Fig. 2a, in10 min, when the stirring intensity increased from 300 to 400 r/min, the removal efficiency of BDE209 was enhanced from 78.9 to 85.4%. However, as the stirring rate further raised to 500 r/min, the degradation efficiency dropped to 54.0%. The removal efficiency of BDE209 increased to 87.7, 93.7, and 93.9% after 60 min, respectively. A hundred percent degradation of BDE209 was achieved after 180 min. When the synthesis stirring rate of Ni/Fe nanoparticles was 400 r/min, the pseudo-first order rate constant (Supporting information) for BDE209 degradation was 0.049 min^{-1}, which was 1.6 times and 1.1 times higher than that of Ni/Fe nanoparticle prepared at 300 r/min (0.031 min^{-1}) and 500 r/min (0.045 min^{-1}), respectively. The reactivity of Ni/Fe bimetallic nanoparticles increased with the increase of stirring rate from 300 to 400 r/min during the synthesis process of Ni/Fe nanoparticles. However, further increasing the stirring rate might reduce the reactivity of Ni/Fe nanoparticles.

As the synthesis stirring rate increased from 300 to 400 r/min, the volume weighted hydrodynamic diameter of Ni/Fe dramatically reduced from 98.32 ± 0.8 to 21.26 ± 0.5 nm and increased to 93.79 ± 1.4 nm. The DLS particle size increased to as the synthesis stirring rate further increased to 500 r/min (Fig. 2b). The results were consistent with the zeta potential analysis (Fig. 2c), which were − 21.21, − 23.31, and − 22.16 mV, respectively, for the nanoparticles prepared at the synthesis stirring speed of 300, 400, and 500 r/min. During the synthesis of Ni/Fe nanoparticles, stirring not only mixed the solution and enhanced the efficiency of heat transfer but also enhanced the dispersion, which had greater effect on the size distribution of nanomaterial. Ni/Fe bimetallic nanoparticles exhibited a strong tendency to agglomerate into larger particles, due to Brownian motion and magnetic forces. The lower the synthesis stirring intensity was, the smaller the shearing force of vortex was, which was difficult to prevent agglomeration of nanoparticles. With the increase of the stirring rate, the shear force produced by stirring and molecule Brownian motion as well as the magnetic forces of nanoparticles were stated in dynamic equilibrium, leading to the uniform size distribution of Ni/Fe

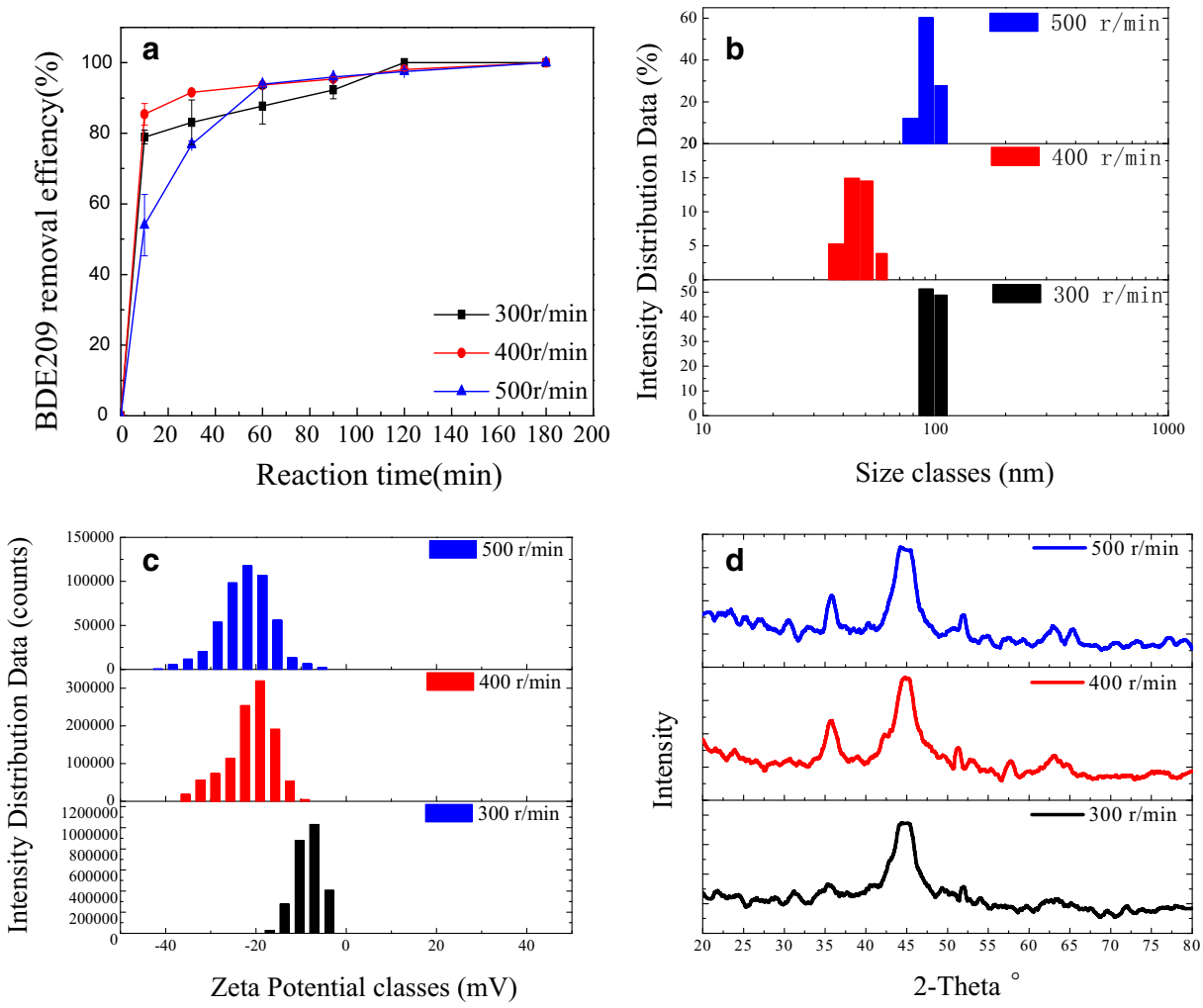

Fig. 2 Effects of stirring rate on the characteristics and reactivity of the Ni/Fe (removal efficiency (**a**), size distribution (**b**), zeta potential (**c**), and XRD (**d**))

nanoparticles. Nevertheless, when the synthesis stirring speed further increased, the shear force also increased, and the dynamic balance was destroyed, as a result, the size distribution of the nanoparticles became broad and non-uniform. Similar results were also reported by An et al. (2010). Considering both characteristics and reactivity of Ni/Fe nanoparticles, the stirring rate was selected at 400 r/min in our study.

XRD patterns (Fig. 2d) of Ni/Fe nanoparticles showed that an apparent peak of Fe^0 ($2\theta = 44.9°$) was present in Ni/Fe with severe background noises, regardless of synthesis stirring rate, showing that amorphous alloy structure of Ni/Fe bimetallic nanoparticles should not be significantly varied by stirring intensively (Fang et al. 2011; Kim et al. 2013; Weng et al. 2013). In addition, the peak at $2\theta = 35.6°$ implied the presence of Fe_3O_4 or γ-Fe_2O_3, which suggested that iron oxides were formed during the preparation or characterization.

3.3 Effects of Washing Solvents

The reactivity and characteristics of Ni/Fe prepared with different washing solvents under otherwise identical conditions are compared in Fig. 3. As shown in Fig. 3a, the removal efficiency of BDE209 was 22.3% (washing by ethanol), 85.4% (washing by ethanol and deoxygenated water), and 38.5% (washing by deoxygenated water), respectively, after 10 min. When the reaction time increased to

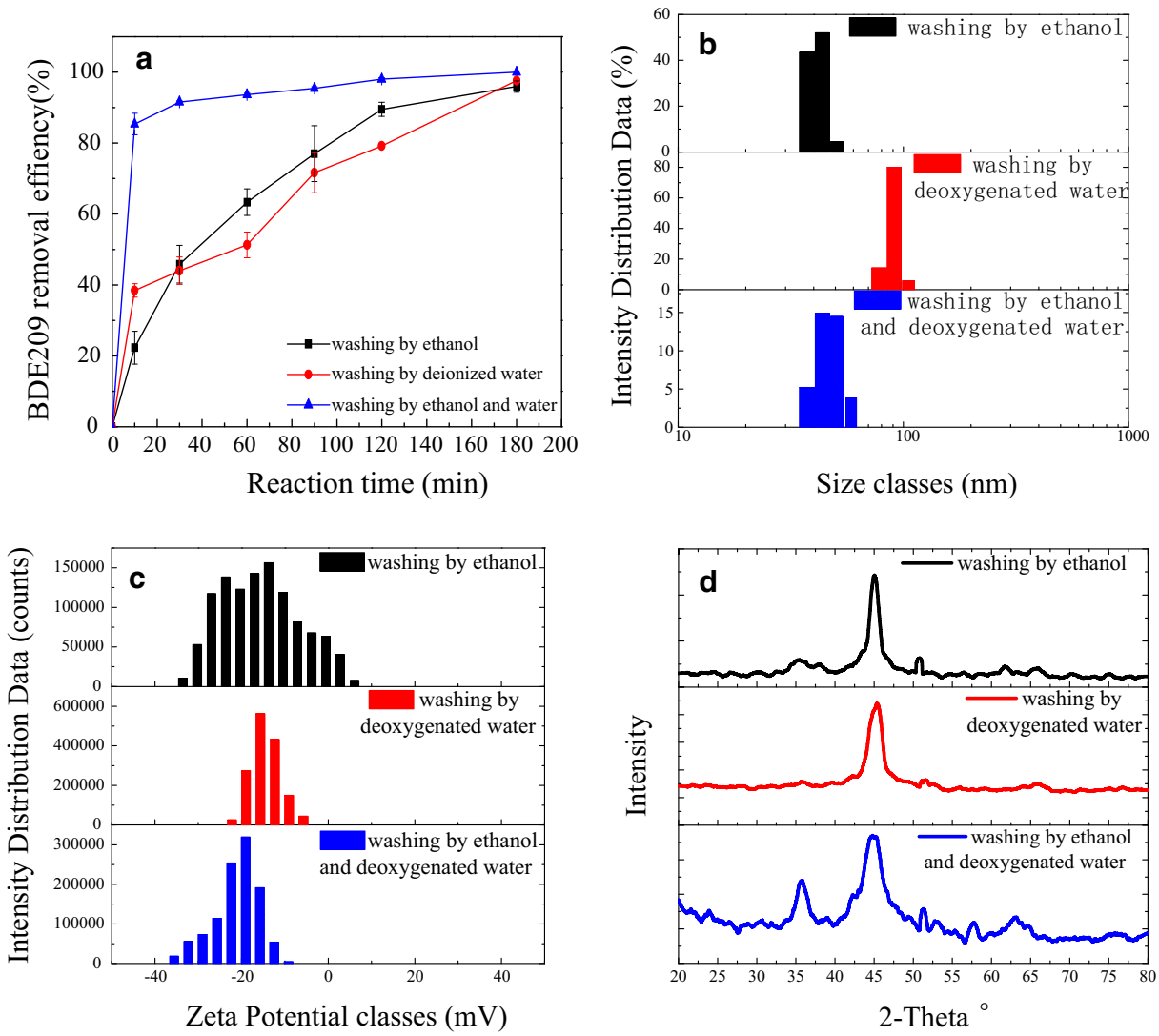

Fig. 3 Effects of washing solvents on the characteristics and reactivity of the Ni/Fe (removal efficiency (**a**), size distribution (**b**), zeta potential (**c**), and XRD (**d**))

60 min, the removal efficiency of BDE209 was enhanced to 63.3, 93.7, and 51.3%, respectively. After 180 min, the efficiency reached 95.9, 100, and 97.6%, respectively. Correspondingly, the reaction rate constants (Supporting information) were 0.018 min^{-1} (washing by ethanol), 0.049 min^{-1} (washing by ethanol and deoxygenated water), and 0.016 min^{-1} (washing by deoxygenated water), which indicated that different washing solutions notably affected the reactivity of the Ni/Fe nanoparticles. The DLS particle size (Fig. 3b) analysis for Ni/Fe gave the average particle size of 90.33 ± 0.2 nm for deoxygenated water, 41.53 ± 1.2 nm for ethanol, and 21.26 ± 0.5 nm for ethanol and deoxygenated water. Zeta potential of Ni/Fe nanoparticles were also measured (Fig. 3c). The absolute values of zeta potential were 14.44, 15.57, and 23.31 mV, respectively. Those findings suggested that different washing solvents significantly affected the particle size distribution and chemical stability of Ni/Fe. Subsequently, the reactivity of Ni/Fe were influenced. During the preparation process of Ni/Fe, excess chemicals could be adored on the surface of nanoparticles; therefore, the washing process was required to rinse out the impurities. Yaacob et al. (2012) found that color, particles size, and texture of nZVI were affected by

washing solutions. Woo et al. (2014) reported that washing with volatile solvents and drying under anaerobic condition decreased the thickness of Fe-oxide layer on nZVI, which enhanced the reactivity of nZVI. The XRD pattern of the Ni/Fe nanoparticles confirmed the formation of iron in their zero-valent state with the major peak at $2\theta = 44.9°$ (Fig. 3d) (Fang et al. 2011; Kim et al. 2013). The nanocrystal displayed peak broadening, which was amorphous structure and consistent with current report (Weng et al. 2013). It was verified that the crystallinity of Ni/Fe were not affected by the different washing solutions.

3.4 Effects of the Ni/Fe Nanoparticle Preparation Methods

Based on the optimized synthesis conditions (synthesis temperature = 40 °C, synthesis stirring = 400 r/min, washing solutions = deoxidizing water and ethanol), Ni/Fe nanoparticles were prepared via two different synthesis methods, namely, post-coated and co-reducted methods. BDE209 removal experiments were conducted using these two types of particles to compare their reactivity. Figure 4a shows that BDE209 removal efficiency by post-coated Ni/Fe nanoparticles was 85.4%, compared to 11.1% by co-

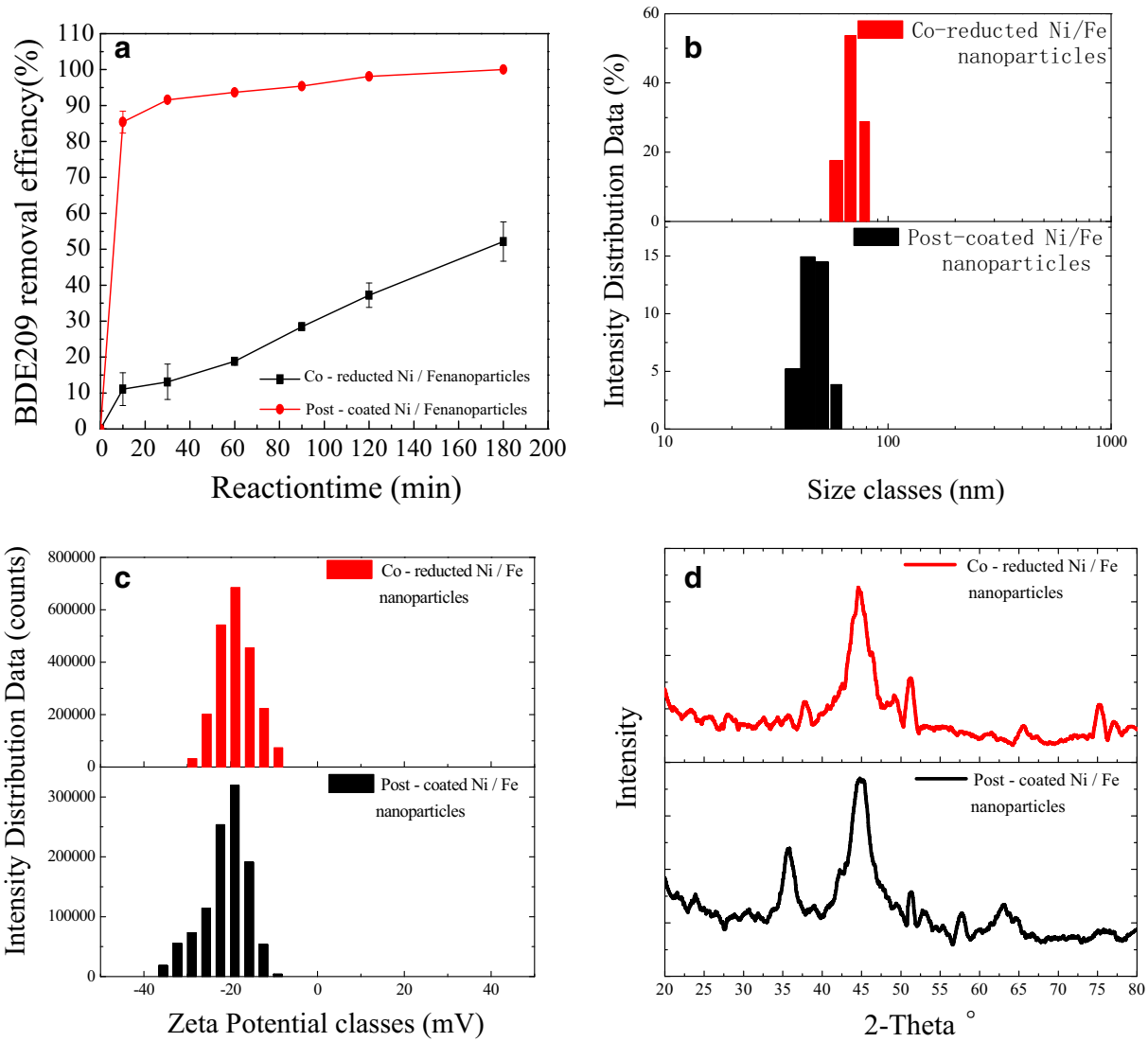

Fig. 4 Effects of preparing methods on the characteristics and reactivity of the Ni/Fe (removal efficiency (**a**), size distribution (**b**), zeta potential (**c**), and XRD (**d**))

reducted Ni/Fe nanoparticles after 10 min. After 180 min, the removal efficiency of BDE209 by post-coated Ni/Fe nanoparticles achieved 100%, which was nearly two times of that by co-reducted Ni/Fe nanoparticles (52.1%). In addition, the kinetics constants (Supporting information) was0.049 min^{-1} for post-coated Ni/Fe nanoparticles, which was approximately 14 times higher than that of co-reducted Ni/Fe nanoparticles. The results showed that the post-coated Ni/Fe nanoparticles method exhibited much higher reactivity than the co-reducted Ni/Fe nanoparticles. The results showed that the Post-coated Ni/Fe nanoparticles method showed much higher reactivity than that obtained by the Co-reducted Ni/Fe nanoparticles method.

The particle size (Fig. 4b) and zeta potential (Fig. 4c) of Ni/Fe synthesized by the different method were investigated. The particle size and the zeta potential of post-coated Ni/Fe nanoparticles were 21.26 ± 0.5 nm and 23.31 mV, respectively. In contrast, the particle size and the zeta potential of co-reducted Ni/Fe nanoparticles were 69.53 ± 2.6 nm and 15.57 mV, respectively. The results of other synthesis conditions (post-coated Ni/Fe nanoparticles) show that the particles size of Ni/Fe have little effect on the removal efficiency of BDE209. However, the findings of Wu and Ritchie (2006) found that the size of post-coated Ni/Fe nanoparticles measured by the TEM ranged from 7 to 11 nm, and the co-reducted Ni/Fe nanoparticles had diameters in the range of 11–24 nm. They considered that post-coating was more effective than co-reduction to prepare bimetallic Ni/Fe nanoparticles with high reactivity. So, we speculated that the size of nanoparticles has a great effect on the reactivity of Ni/Fe nanoparticles prepared by different synthesis methods.

XRD patterns of Ni/Fe nanoparticles prepared by different method are shown in Fig. 4d. Characteristic peak of $2\theta = 44.9°$ indicates the crystallization of Fe^0 in Ni/Fe, an additional peak appeared at 35.6° on the particles, indicating the formation of γ-Fe_2O_3 or Fe_3O_4 during the reaction or synthesis; moreover, the nanocrystal displayed peak were broadening, which indicated these nanoparticles were formed as an amorphous phase (Petersen et al. 2012; Woo et al. 2014; Hu et al. 2016). Therefore, according to the analysis results, the influence of different preparation methods of Ni/Fe on the crystal structure were neglectable.

4 Conclusions

In this study, effects of synthesis temperature, stirring rate, washing solutions, and preparation methods on the reactivity and characteristics of Ni/Fe nanoparticles were investigated. Results showed that synthesis conditions not only clearly affected the particle size and zeta potential of Ni/Fe but also had impacts on the removal efficiency of BDE209. However, the influence of synthesis conditions on the crystalline structure of Ni/Fe was neglectable. The optimization of synthesis conditions of Ni/Fe nanomaterials may facilitate their more effective application for organic contaminant degradation.

Acknowledgments The authors acknowledge the financial support from the Joint Foundation of NSFC-Guangdong Province (Grant No. U1401235) and Guangdong Province Environment Remediation Industry Technology Innovation Alliance.
(Grant No. 2017B090907032).

Compliance with Ethical Standards

Conflict of Interest The authors declare that they have no conflict of interest.

References

Alowitz, M. J., & Scherer, M. M. (2002). Kinetics of nitrate, nitrite and Cr(VI) reduction by iron metal. *Environmental Science & Technology, 36*(3), 299–306.

An, B., Cai, X. H., Wu, F. S., & Wu, Y. P. (2010). Preparation of micro-sized and uniform spherical Ag powders by novel wet-chemical method.Transactions of. *Nonferrous Metals Society of China, 20*(8), 1550–1554.

Bae, S., & Lee, W. (2014). Influence of riboflavin on nanoscale zero-valent iron reactivity during the degradation of carbon tetrachloride. *Environmental Science & Technology, 48*(4), 2368–2376.

Chen, S., Qin, Z. L., Quan, X., Zhang, Y. B., & Zhao, H. M. (2010). Electrocatalyticdechlorination of 2,4,5-trichlorobiphenyl using an aligned carbon nanotubes electrode deposited with palladium nanoparticles. *ChineseScience Bulletin, 55*(4–5), 358–364.

Choe, S. H., Liljestr, H. M., & Khim, J. (2004). Nitrate reduction by zero-valent iron under different pH regimes. *AppliedGeochemistry, 19*(3), 335–342.

Chun, C. L., Baer, D. R., Matson, D. W., Amonette, J. E., & Penn, R. L. (2010). Characterization and reactivity of iron nanoparticles prepared with added Cu, Pd, and Ni. *Environmental Science & Technology, 44*, 5079–5085.

Fang, Z. Q., Qiu, X. H., Chen, J. H., & Qiu, X. Q. (2011). Debromination of polybrominateddiphenyl ethers by Ni/Fe bimetallic nanoparticles: influencing factors, kinetics, and

mechanism. *Journal of Hazardous Materials, 185*(2–3), 958–969.

He, F., & Zhao, D. Y. (2007). Manipulating the size and dispersibility of zerovalent iron nanoparticles by use of carboxymethylcellulose stabilizers. *Environmental Science & Technology, 41*(17), 6216–6221.

Hu, S. H., Zhang, C. J., Yao, H. R., Lu, C., & Wu, Y. G. (2016). Intensify chemical reduction to remove nitrate from groundwater via internal microelectrolysis existing in nano-zero valent iron/granular activated carbon composite. *Desalination and Water Treatment, 57*(30), 14158–14168.

Hwang, Y. H., Kim, D. G., & Shin, H. S. (2011). Effects of synthesis conditions on the characteristics and reactivity of nano scale zero valent iron. *Applied Catalysis B: Environmental, 105*(1–2), 144–150.

Kim, S. A., Kannan, S. K., Lee, K. J., Park, Y. J., Shea, P. J., Lee, W. H., Kim, H. M., & Oh, B. T. (2013). Removal of Pb(II) from aqueous solution by azeolite-nanoscale zero-valent iron composite. *Chemical Engineering Journal, 217*, 54–60.

Leal, J. F., Esteves, V. I., & Santos, E. B. H. (2013). BDE-209: kinetic studies and effect of humic substances on photodegradation in water. *Environmental Science & Technology, 47*(24), 14010–14017.

Li, L., Fan, M. H., & Brown, R. C. (2006). Synthesis, properties, and environmental applications of nanoscale iron-based materials: a review. *Critical Reviews in Environmental Science and Technology, 36*, 405–431.

Li, X. Q., & Zhang, W. X. (2007). Sequestration of metal cations with zero valent iron nanoparticles—a study with high resolution X-ray photoelectron spectroscopy (HR-XPS). *Journal of Physical ChemistryC, 111*(19), 6939–6946.

Lin, C. H., Shih, Y. H., & MacFarlane, J. (2015). Amphiphilic compounds enhance the dechlorination of pentachlorophenol with Ni/Fe bimetallic nanoparticles. *Chemical Engineering Journal, 262*, 59–67.

Liou, Y. H., Lo, S. L., Kuan, W. H., Lin, C. J., & Weng, S. C. (2006). Effects of precursor concentration on the characteristics of nanoscalezerovalent iron and its reactivity of nitrate. *Water Research, 40*(13), 2485–2492.

Petersen, E. J., Pinto, R. A., Shi, X. Y., & Huang, Q. G. (2012). Impact of size and sorption on degradation of trichloroethylene and polychlorinated biphenyls by nano-scale zerovalent iron. *Journal of Hazardous Materials, 243*, 73–79.

Ponder, S. M., & Mallouk, T. E. (2000). Remediation of Cr(VI) and Pb(II) aqueous solution using supported nanoscalezerovalentiron. *Environmental Science & Technology, 34*(12), 2564–2569.

Shen, W. J., Mu, Y., Wang, B. N., Ai, Z. H., & Zhang, L. Z. (2017). Enhanced aerobic degradation of 4-chlorophenol with iron-nickel nanoparticles. *Applied Surface Science, 393*, 316–324.

Tan, L., Lu, S. Y., Fang, Z. Q., Cheng, W., & Tsang, E. P. (2017). Enhanced reductive debromination and subsequent oxidative ring-opening of decabromodiphenyl ether by integrated catalyst of nZVI supported on magnetic Fe_3O_4 nanoparticles. *Applied Catalysis B: Environmental, 200*, 200–210.

Tian, H., Li, J. J., Mu, Z., Li, L. D., & Hao, Z. P. (2009). Effect of pH on DDT degradation in aqueous solution using bimetallic Ni/Fe nanoparticles. *SeparationandPurificationTechnology, 66*(1), 84–89.

Wang, W., Hua, Y. L., Li, S. L., Yan, W. L., & Zhang, W. X. (2016). Removal of Pb(II) and Zn(II) using lime and nanoscale zero-valent iron (nZVI): a comparative study. *Chemical Engineering Journal, 304*, 79–88.

Weng, X. L., Lin, S., Zhong, Y. H., & Chen, Z. L. (2013). Chitosan stabilized bimetallic Fe/Ni nanoparticles used to remove mixed contaminants-amoxicillin and Cd (II) from aqueous solutions. *Chemical Engineering Journal, 229*, 27–34.

Woo, H., Park, J., & Lee, S. (2014). Effects of washing solution and drying condition on reactivity of nano-scale zero valent irons (nZVIs) synthesized by borohydride reduction. *Chemosphere, 97*, 146–152.

Wu, L. F., & Ritchie, S. M. C. (2006). Removal of trichloroethylene from water by cellulose acetate supported bimetallic Ni/Fe nanoparticles. *Chemosphere, 63*(2), 285–292.

Xie, Y. Y., Fang, Z. Q., Cheng, W., Tsang, P. E., & Zhao, D. Y. (2014). Remediation of polybrominateddiphenyl ethers in soil using Ni/Fe bimetallic nanoparticles: influencing factors, kinetics and mechanism. *Science of the Total Environment, 85*, 363–370.

Yaacob, W. Z. W., Kamaruzaman, N., & Rahim, A. (2012). Development of nano-zero valent iron for the remediation of contaminated water. *Chemical Engineering Transactions, 28*, 25–30.

Yang, Z. L., Zhai, D. D., Wang, X., & Wei, J. (2014). In situ synthesis of highly monodispersednonaqueous small-sized silver nano-colloids and silver/polymer nanocomposites by ultraviolet photo polymerization. *Colloids and Surfaces A: Physicochemical and Engineering Aspects, 448*, 107–114.

Yazdanbakhsh, A. R., Daraei, H., Rafiee, M., & Kamali, H. (2016). Performance of iron nano particles and bimetallic Ni/Fe nanoparticles in removal of amoxicillintrihydrate from synthetic wastewater. *Water Science & Technology, 73*(12), 2998–3007.

Zhang, Z., Cissoko, N., Wo, J., & Xu, X. J. (2009). Factors influencing the dechlorination of 2,4-dichlorophenol by Ni-Fe nanoparticles in the presence of humic acid. *Journal of Hazard Materials, 165*, 78–86.

Zhang, W. H., Quan, X., Wang, J. X., Zhang, Z. Y., & Chen, S. (2006). Rapid and complete dechlorination of PCP in aqueous solution using Ni-Fe nanoparticles under assistance of ultrasound. *Chemosphere, 65*(1), 58–64.

Zhuang, Y., Ahn, S., & Luthy, R. G. (2010). Debromination of polybrominateddiphenylethers by nanoscalezerovalentiron: pathways, kinetics, and reactivity. *Environmental Science & Technology, 44*(21), 8236–8242.